Spheromak Formation by Steady Inductive Helicity Injection

T. R. Jarboe, W. T. Hamp, G. J. Marklin, B. A. Nelson, R. G. O'Neill, A. J. Redd, P. E. Sieck, R. J. Smith, and J. S. Wrobel
University of Washington, Seattle, Washington 98195-2250, USA
(Received 1 February 2006; published 15 September 2006)

A spheromak is formed for the first time using a new steady state inductive helicity injection method. Using two inductive injectors with odd symmetry and oscillating at 5.8 kHz, a steady state spheromak with even symmetry is formed and sustained through nonlinear relaxation. A spheromak with about 13 kA of toroidal current is formed and sustained using about 3 MW of power. This is a much lower power threshold for spheromak production than required for electrode-based helicity injection. Internal magnetic probe data, including oscillations driven by the injectors, agree with the plasma being in the Taylor state. The agreement is remarkable considering the only fitting parameter is the amplitude of the spheromak component of the state.

DOI: 10.1103/PhysRevLett.97.115003 PACS numbers: 52.55.Wq, 52.35.Vd, 52.55.Ip

Magnetic helicity, the self-linkage of magnetic flux, is the best constant of motion for magnetized plasma in resistive magnetohydrodynamics [1]. Helicity is conserved on the time scales of energy dissipating instabilities, and, on these time scales, magnetic configurations relax toward the state of minimum energy that conserves helicity (MECH state) [2]. Only collisional resistive processes dissipate helicity [3]. Thus, to sustain a helicity containing magnetic structure for times longer than the resistive decay time, helicity must be injected. Since relaxation is on a shorter time scale than resistive decay, relaxation will maintain the configuration even if the helicity is injected with a different topology than that of the relaxed state [4]. Helicity injection, using coaxial electrodes (CHI), has been used to form and sustain spheromaks [5–9] and spherical tori [10–14]. Helicity conservation has been confirmed experimentally [15].

The spheromak is the minimum energy state for an oblate-shaped spheroidal volume [16]. This equilibrium can have closed nested flux surfaces that should have good confinement with no material or coils linking the boundary. Thus, from an engineering point of view, it leads to a smaller, much more cost effective reactor compared to configurations that have a toroidal vacuum vessel linked by large toroidal field coils [17]. With a boundary having a bowtie-shaped cross section and helicity injection driving the edge, β limits of 10% are possible [18]. However, the confinement must be sufficient so that the β limit will be reached.

Decaying CHI produced spheromaks have adequate confinement [19,20]. Ohmic heating to the β limit [21] and temperatures of several hundred electron volts have been achieved [20,22]. However, CHI sustained spheromaks have not achieved such results. To eliminate electrodes and open field lines, the helicity injected torus with steady inductive helicity injection (HIT-SI) has been built [23–25] to form and sustain a spheromak inductively. This Letter reports the first spheromak production and sustainment in HIT-SI. The power required is only 3 MW, more than an order of magnitude lower than required for CHI spheromak production [26].

Figure 1 shows a cross section of the HIT-SI device. The experiment has a bowtie-shaped spheromak confinement region with two helicity injectors. The injectors are 180° segments of a small, elongated cross section reversed field pinch. In each injector, the loop voltage and toroidal flux are oscillated in phase at 5.8 kHz. This frequency is low enough so that the circulating power in the toroidal flux circuit is manageable and high enough so that the V sec requirement of the loop voltage is acceptable. The injectors are 90° out of phase with voltage and flux amplitudes of V_0 and ψ_0. This gives a constant helicity injection rate of $2V_0\psi_0$ [23]. References [24,25] give a more detailed discussion of HIT-SI and its operation.

With flux boundary conditions, the MECH state is the Taylor state and is found by solving $\nabla \times \mathbf{B} = \lambda \mathbf{B}$ inside

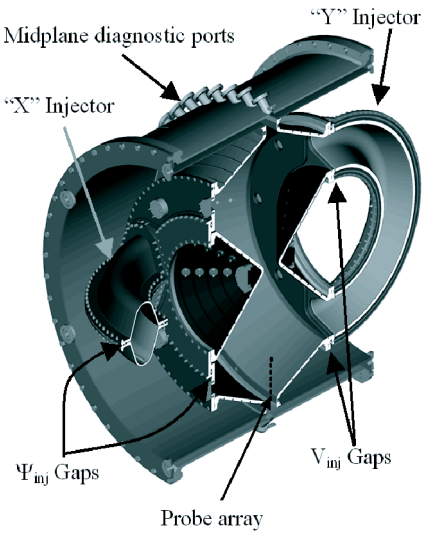

FIG. 1 (color online). Cross section of the HIT-SI copper shell and insulating breaks used for steady inductive helicity injection. The locations of the magnetic probes of the probe array are shown. The toroidal grooves for the flux loops are shown.

the boundary where λ is a global constant [27]. In HIT-SI with no flux in the injectors, the Taylor state is a spheromak, having even symmetry in x and y, that is mostly $n = 0$ with a small amount of $n = 2$, and the eigenvalue (λ_{sph}) is 10.4 m^{-1}. Adding toroidal flux in an injector allows any value of the injector $\lambda(\lambda_{inj})$ to satisfy $\nabla \times \mathbf{B} = \lambda \mathbf{B}$ in the entire volume with odd symmetry in either x or y. At small amounts of helicity, λ is less than λ_{sph} and there is no spheromak current. As more helicity is added, λ increases until it reaches λ_{sph}. When the helicity exceeds this value, the spheromak forms, and a further increase in the system helicity leads to an increase in the spheromak fields without a change in λ. Thus, when the helicity content is high enough to form a spheromak, the Taylor state of HIT-SI has three components: an odd component from each injector, with their flux having just enough current so that λ_{inj} in each is equal to λ_{sph}, and an even component, the spheromak, that has the amplitude needed to contain the remaining helicity. Figure 2(a) shows the magnetic field lines of the injector Taylor state when λ_{inj} equals λ_{sph} [28].

The superposition of Taylor states of equal λs is still a Taylor-state equilibrium. The injectors have odd symmetry in x or y and solving $\nabla \times \mathbf{B} = \lambda \mathbf{B}$, with $\lambda = 10.4$ m^{-1}, in the injectors does not couple to the even-symmetry spheromak. (In CHI, solving $\nabla \times \mathbf{B} = \lambda \mathbf{B}$, with $\lambda_{inj} = \lambda_{sph}$, gives infinite spheromak helicity because the injector and spheromak both have even symmetry.) Thus, by adding the spheromak state to the injector states, Taylor states with any ratio of injector current to spheromak current can be calculated. Figure 2(b) shows the field lines of a Taylor state with the ratio approximately equal to that observed so far. Figure 2(c) shows what might be achieved with more optimization on HIT-SI. Figures 2(b) and 2(c) have an isolated closed flux region that is surrounded by edge field lines that pass through the injectors. Thus, these Taylor states have the proper topology for good plasma confinement. The threshold for this separatrix formation is about where the spheromak toroidal current is equal to the amplitude of the injector currents.

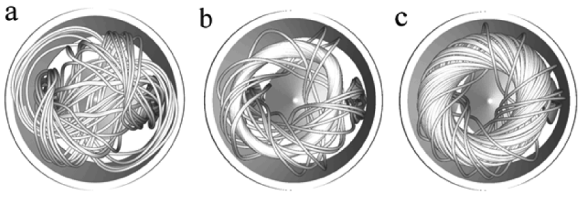

FIG. 2. Magnetic fields of Taylor states with different amounts of spheromak current compared to the injector current. In (a), the spheromak current is zero and only the injector Taylor state is shown. In (b), spheromak toroidal currents are 1.5 times that of the amplitude of the injectors. In (c), the spheromak toroidal current is 5 times the injector amplitude. For all figures, the phase is such that the shown injector is at the maximum current and flux and the other is at zero. All phases look qualitatively similar except, of course, for the amount of flux that links each injector.

The measurement results given in this Letter are from internal magnetic probes and flux loops external to the copper shell. (Both have at least 3% accuracy.) Figure 1 shows the location of the magnetic probe coils. The 20 flux loops are mounted in the toroidal grooves in the outside surfaces of the flux conserver of the bowtie spheromak region, shown in Fig. 1. Assuming the flux conserver is thin and the magnetic field is zero on the outside, the poloidal magnetic field on the inside can be calculated from the rate of flux loss and the surface resistance of the flux conserver. It is given by $B_{pol} = (\mu_0 \delta / 2\pi R \eta) d\psi/dt$, where δ is the thickness of the flux conserver, R is the radius of the flux conserver, η is the resistivity of the flux conserver material, and ψ is the poloidal flux that has resistively diffused out of the flux conserver. The flux conserver is 12.7 mm thick chromium copper with 80% the conductivity of pure copper. Figure 3 shows the injector parameters as a function of time during shot no. 104338. The voltage and flux are feedback controlled by pulse width modulation. The amplitude of the flux demand curve is a function of time in order to keep λ_{inj} as close as practical to 17 m^{-1}. The demand shape is determined from previous nearly identical shots. In practice, λ_{inj} must be greater than λ_{sph} so there is free energy to drive relaxation [29].

Figure 4(a) shows the total power injected as a function of time. A flux loop signal is shown in Fig. 4(b), which gives a rate of loss of about 30 mW b/ sec, which is used to

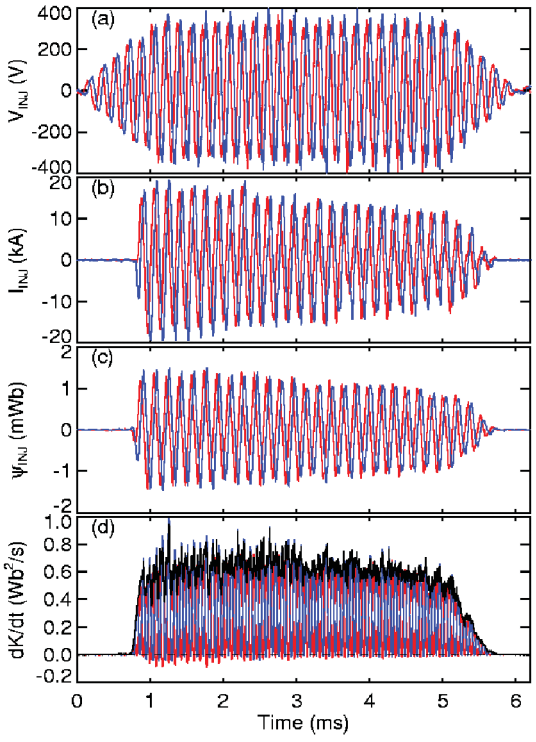

FIG. 3 (color). Injector parameters as a function of time: red for the X injector and blue for the Y injector. (a) Loop voltage. (b) Toroidal current. (c) Toroidal flux. (d) Helicity injection rate with black as the total of both injectors.

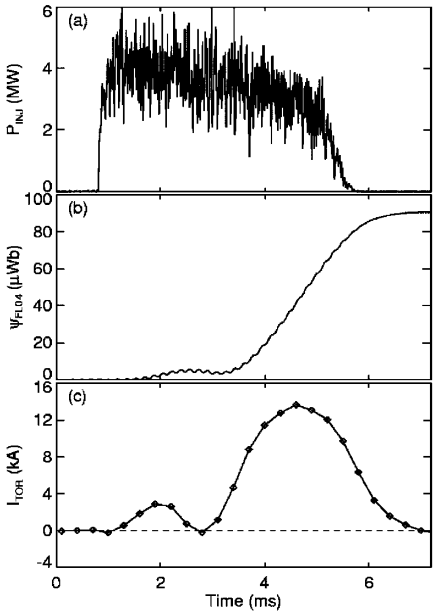

FIG. 4. Spheromak parameters as a function of time. (a) Total input power. (b) Typical flux loss out of the shell as a function of time. (c) Toroidal ($n = 0$) spheromak current as a function of time.

find B_{pol} at the positions of the flux loops. Ampere's law is then used around the inside of the poloidal perimeter to calculate the toroidal current, assuming B_{pol} is equal to that measured by the nearest flux loop. Figure 4(c) shows the plasma current as a function of time. At its peak, the spheromak current is about 13.7 kA. A spheromak is formed only if both injectors inject the same sign of helicity; the flux and voltage are within 30° of being in phase on both injectors; the power is above 2 MW and the wall conditions are clean (base pressure low 10^{-8} torr). The direction of the spheromak current reverses when the rotation of the injector driven structure is reversed. Figure 5 shows the toroidally averaged surface poloidal field on the flux conserver as deduced from the flux loop data, at the peak of the toroidal current. Also shown are the Taylor-state values for the spheromak with the best least squares fit to the data, yielding 11.8 kA of toroidal spheromak current.

Data from internal magnetic field probes are shown in Figs. 6 and 7. The positions of the probes are shown in Fig. 1. There are three overlaying traces at each position for poloidal and toroidal fields. The two black overlaying traces are the probe data with different low pass filters. One filter is at essentially the full bandwidth of the probe, 200 kHz. The other is heavily filtered at 1.5 kHz to eliminate most of the 5.8 kHz signal produced by the oscillating injectors, revealing the ''steady state'' component.

Note that, slightly before 3 ms, a steady state component begins to grow. In the poloidal field, the steady state component at the wall exceeds the amplitude of the 5.8 kHz oscillation and the fields become unidirectional. For the toroidal field, the same behavior occurs but for the positions furthest from the wall. The red traces are from the

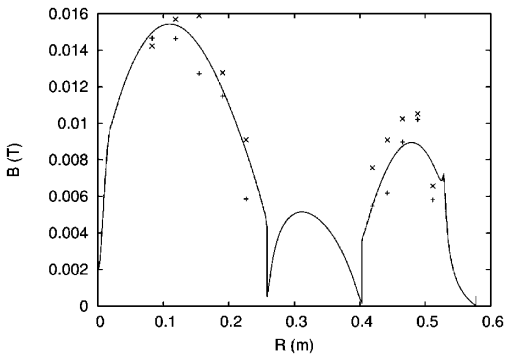

FIG. 5. Plot of the poloidal magnetic field on the wall of the flux conserver as a function of the major radius. The data shown are from flux loop data. Data from the X half of the flux conserver are shown with pluses (+) and data from the Y half are shown with crosses (×). The solid curve is for the poloidal field at the wall of the Taylor-state spheromak.

composite Taylor state, which is the sum of each injector state, having the measured injector current, and the spheromak state. The amplitude of the spheromak state at 4.5 ms is found by doing a least squares fit to the steady state poloidal and toroidal fields at that time. This yields a spheromak state with a toroidal current of 12.3 kA, which is about 123% of the injector current. For other times, these spheromak fields are multiplied by a scale factor equal to the toroidal field measured at $R = 0.387$ m divided by its value there at 4.5 ms. Thus, this method of fitting assures only fairly good agreement between the steady state values

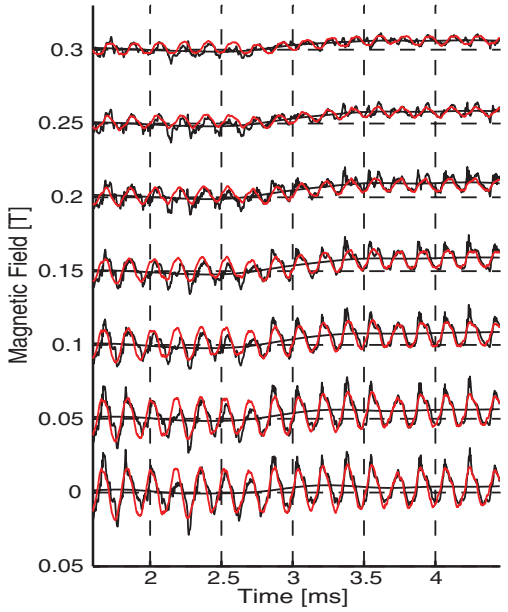

FIG. 6 (color). Internal poloidal magnetic field for shot no. 104338 as a function of time. The Taylor-state model predicts the red lines. From top to bottom, the major radii of the probe positions are 0.514, 0.489, 0.464, 0.438, 0.413, 0.387, and 0.362 m. The traces are offset for clarity, and the zero magnetic field value for each trace is at the nearest horizontal dashed line.

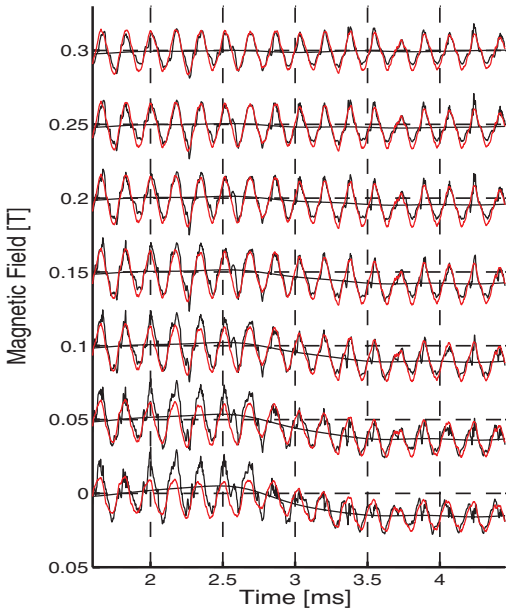

FIG. 7 (color). Internal toroidal magnetic field for shot no. 104338 as a function of time. The presentation of the data is the same as in Fig. 6.

of the model and the experiment for the toroidal field data at $R = 0.387$ m. The agreement of the steady state values of all other traces depends on the accuracy of the Taylor state in representing the experiment.

The model nearly matches the probe data and lets us understand the gross features of the equilibrium. It shows good agreement with the amplitude of the injector driven fluctuations for all of the probe data. The phase of the fluctuations is in fair agreement for both the toroidal field and the poloidal field. The steady state spheromak component agrees well with the toroidal field at all major radii, which may be due, in part, to forced agreement at $R = 0.387$ m. On the poloidal data, the magnetic fields agree fairly well. The poloidal data indicate that the magnetic axis has approximately the same radius as the Taylor state. These results clearly demonstrate that steady inductive helicity injection with odd symmetry can form and sustain a spheromak. However, the formation of a separatrix is still not proven because $I_{\mathrm{sph}}/I_{\mathrm{inj}}$ is barely above the required threshold and the equilibrium is not perfectly in the Taylor state. The lifetime of the spheromak is not understood at this time, and it is not increased when the power is kept on for a longer time. While the density was not measured, similar discharges had far-infrared-interferometer measured densities from a few to several times 10^{19} m^{-3}. The electron temperature has not been measured, but similar spheromaks have had temperatures well under 100 eV.

[1] J. W. Edenstrasser, Phys. Plasmas **2**, 1206 (1995).
[2] J. B. Taylor, Rev. Mod. Phys. **58**, 741 (1986).
[3] T. R. Jarboe, Plasma Phys. Controlled Fusion **36**, 945 (1994).
[4] J. C. Fernández *et al.*, Phys. Fluids B **1**, 1254 (1989).
[5] T. R. Jarboe *et al.*, Phys. Rev. Lett. **51**, 39 (1983).
[6] H. S. McLean, Phys. Rev. Lett. **88**, 125004 (2002).
[7] R. C. Duck *et al.*, Plasma Phys. Controlled Fusion **39**, 715 (1997).
[8] A. al-Karkhy *et al.*, Phys. Rev. Lett. **70**, 1814 (1993).
[9] M. R. Brown *et al.*, Astrophys. J. **577**, L63 (2002).
[10] T. R. Jarboe *et al.*, Phys. Plasmas **5**, 1807 (1998).
[11] B. A. Nelson *et al.*, Phys. Plasmas **2**, 2337 (1995).
[12] R. Raman *et al.*, Nucl. Fusion **41**, 1081 (2001).
[13] M. Nagata *et al.*, Phys. Plasmas **10**, 2932 (2003).
[14] K. J. Gibson *et al.*, Plasma Phys. Controlled Fusion **42**, 1331 (2000).
[15] C. W. Barnes *et al.*, Phys. Fluids **29**, 3415 (1986).
[16] M. N. Rosenbluth and M. N. Bussac, Nucl. Fusion **19**, 489 (1979).
[17] R. L. Hagenson and R. A. Krakowski, Fusion Technol. **8**, 1606 (1985).
[18] U. Shumlak and T. R. Jarboe, Phys. Plasmas **7**, 2959 (2000).
[19] F. J. Wysocki *et al.*, Phys. Rev. Lett. **65**, 40 (1990).
[20] D. R. Wood *et al.*, Nucl. Fusion **45**, 1582 (2005).
[21] F. J. Wysocki *et al.*, Phys. Rev. Lett. **61**, 2457 (1988).
[22] T. R. Jarboe *et al.*, Phys. Fluids B **2**, 1342 (1990).
[23] T. R. Jarboe, Fusion Technol. **36**, 85 (1999).
[24] P. E. Sieck *et al.*, IEEE Trans. Plasma Sci. **33**, 723 (2005).
[25] P. E. Sieck *et al.*, Nucl. Fusion **46**, 254 (2006).
[26] C. W. Barnes *et al.*, Phys. Fluids B **2**, 1871 (1990).
[27] L. Woltjer, Proc. Natl. Acad. Sci. U.S.A. **44**, 489 (1958).
[28] Homogeneous Taylor states are computed by minimizing the Rayleigh quotient

$$R(\mathbf{A}) = -\int \mathbf{A}\cdot(\nabla\times\mathbf{A})dV/\int(\nabla\times\mathbf{A})^2 dV,$$

on a tetrahedral mesh generated using the T3D code [http://mech.fsv.cvut.cz/~dr/t3d.html]. The curl operators are replaced by finite volume approximations, and the resulting function $R(\mathbf{A}_i)$ is minimized using the conjugate gradient algorithm with the conducting wall boundary condition $\mathbf{A}\times\mathbf{n} = 0$. The minimizing solution will satisfy $\nabla\times\nabla\times\mathbf{A} = \lambda\nabla\times\mathbf{A}$ or $\nabla\times\mathbf{B} = \nabla\times\mathbf{A}$ if $\mathbf{B} = \nabla\times\mathbf{A}$ and $\lambda \equiv -1/R_{\mathrm{min}}$ is the smallest positive eigenvalue. To compute inhomogeneous Taylor states, first compute the vacuum field for each injector $B_v = \nabla\chi$, where the potential χ satisfies a Laplace equation with a jump condition across a gap in the injector set to produce the desired amount of flux. Then minimize the functional

$$F(\mathbf{A}) = \int[(\nabla\times\mathbf{A})^2 - \lambda A\cdot(\nabla\times\mathbf{A}) - 2\lambda\mathbf{A}\cdot\nabla\chi]dV,$$

using the conjugate gradient algorithm with the same mesh, the same finite volume approximation for the curl operators, and the same boundary conditions as before. The minimizing solution will satisfy $\nabla\times\nabla\times\mathbf{A} - \lambda\nabla\times\mathbf{A} = \lambda\nabla\chi$ or $\nabla\times\mathbf{B} = \lambda\mathbf{B}$ if $\mathbf{B} = \nabla\times\mathbf{A} + \nabla\chi$. In this case, however, we may specify any value for λ which is the ratio of current to flux in an injector.
[29] T. R. Jarboe and B. Alper, Phys. Fluids **30**, 1177 (1987).